AGU PUBLICATIONS

Geophysical Research Letters

RESEARCH LETTER
10.1002/2016GL071143

Key Points:
- On Ceres recently exposed materials such as proximal crater ejecta show spectrally bluish characteristic
- Crater ejecta can be dated by measurement of crater size-frequency distributions
- Correlation of color ratios and ejecta formation ages are used to derive a functional relationship for the optical maturation process

Supporting Information:
- Supporting Information S1

Correspondence to:
N. Schmedemann,
nico.schmedemann@fu-berlin.de

Citation:
Schmedemann, N., et al. (2016), Timing of optical maturation of recently exposed material on Ceres, *Geophys. Res. Lett.*, *43*, 11,987–11,993, doi:10.1002/2016GL071143.

Received 11 SEP 2016
Accepted 20 NOV 2016
Accepted article online 1 DEC 2016
Published online 14 DEC 2016

Timing of optical maturation of recently exposed material on Ceres

Nico Schmedemann[1], T. Kneissl[1], A. Neesemann[1], K. Stephan[2], R. Jaumann[1,2], K. Krohn[2], G. G. Michael[1], K. D. Matz[2], K. A. Otto[2], C. A. Raymond[3], and C. T. Russell[4]

[1]Institute of Geological Sciences, Freie Universität Berlin, Berlin, Germany, [2]Institute of Planetary Research, German Aerospace Center, Berlin, Germany, [3]Jet Propulsion Laboratory, California Institute of Technology, Pasadena, California, USA, [4]Institute of Geophysics and Planetary Physics, University of California, Los Angeles, California, USA

Abstract On Ceres, multispectral imaging data from the Dawn spacecraft show a distinct bluish characteristic for recently exposed material from the subsurface in, for example, crater ejecta. Ejecta blankets of presumably old craters show a more reddish spectrum. We selected areas in which fresh material from the Cerean subsurface was exposed at a specific time in the past, and no later geologic process is expected to have changed its surface composition or its cratering record. For each area, we determined two color ratios and the crater retention age. The measured color ratios show an exponential diminishment of the bluish characteristic over time. Although the cause of the color change remains uncertain, the time-dependent change in spectral properties is evident, which could help identify the process.

1. Introduction

The Dawn spacecraft entered orbit around Ceres on 6 March 2015 and mapped Ceres from orbits of three different altitudes with its Framing Camera (FC) [*Sierks et al.*, 2011], Visual and Infrared Spectrometer (VIR) [*De Sanctis et al.*, 2011], and Gamma Ray and Neutron Detector (GRaND) [*Prettyman et al.*, 2011]. The data presented in this work are based on the FC instrument. It features seven color and one clear (panchromatic) filter. Ceres revealed a surface that is more heavily cratered than previously expected [*Bland et al.*, 2016] and less relaxed than other icy bodies [*Jaumann et al.*, 2016], implying a lower fraction of water ice close to the surface. Large impact basins similar to Rheasilvia or Veneneia on Vesta are missing on Ceres [*Hiesinger et al.*, 2016]. The material composition of Ceres' surface material appears to be dominated by phyllosilicates and carbonates [*De Sanctis et al.*, 2016]. The presumably young cryovolcanic dome Ahuna Mons [*Ruesch et al.*, 2016] as well as the possible detection of recent activity within Occator crater [*Nathues et al.*, 2015] may imply that Ceres is a geologically active world.

Preliminary data analysis [*Jaumann et al.*, 2016] showed bluish colors associated predominantly with recently exposed material, such as ejecta blankets and the ejecta rays of large and pristine craters (Figure 1). In general, there appears to be a rough spatial correlation of the bluish material with occurrences of phyllosilicates [*Ammannito et al.*, 2016]. Here we define bluish as a decreasing reflectivity with increasing wavelengths in the visible range between 438 nm and 965 nm. The nature of the bluish material is still under investigation [*Stephan et al.*, 2016]. Measurements of crater size-frequency distributions (CSFDs) of various sample areas showing a more or less bluish characteristic showed a clear correlation between spectral slope and crater retention age [*Jaumann et al.*, 2016]. In this work we specify this correlation by a functional relationship for two different color ratios and 16 sample areas that show the least influence of disturbing processes such as blanketing from adjacent impact craters or blanketing from outgassing events as suggested by *Nathues et al.* [2015]. Optical maturity is a process that is observed on several bodies in the solar system. Depending on the composition of the materials, and the particle and radiation environment, the optical maturation appears to show various results on the investigated planetary bodies [*Pieters and Noble*, 2016]. For instance, a reddening and darkening is observed for iron-bearing powdered surfaces if irradiated with protons [*Hapke*, 1973; *Wehner*, 1964]. Micrometeorite bombardment can produce optically active nanophase iron. If exposed to continuous micrometeorite bombardment, such nanophase iron particles are able to agglutinate and coalesce into larger particles [e.g., *Sasaki et al.*, 2003]. On icy satellites nanophase particle-induced Rayleigh scattering has been suggested as the cause for increased reflectivity in the blue spectral range [*Clark et al.*, 2008]. On Mimas high-energy electron deposition from Saturn's magnetosphere appears to alter the structure of the surficial ice layer, such that the thermal inertia and UV reflectivity is increased

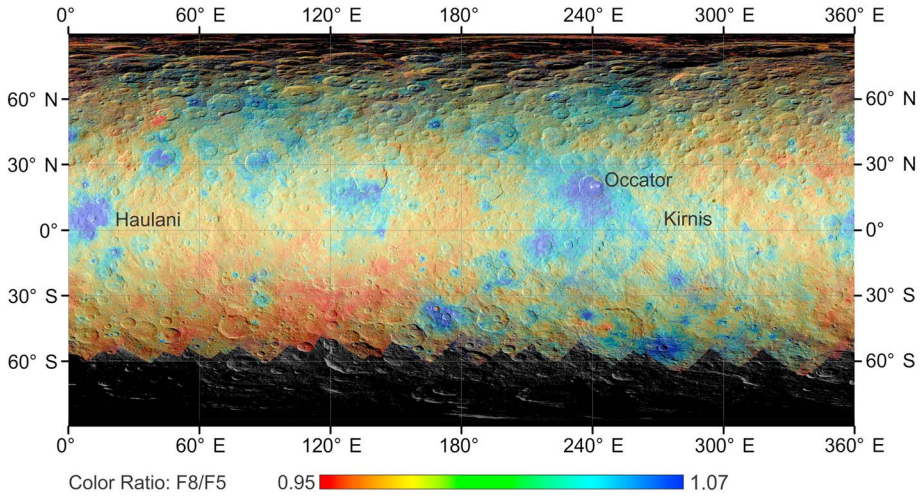

Figure 1. Global map of Ceres. Color ratio F8 (438 nm)/F5 (965 nm) superimposed on clear filter data centered at 180° longitude. Ratios above the average are often correlated with pristine crater ejecta (e.g., at Haulani and Occator craters). Ratios below the average are found in densely cratered areas where ejecta of recently formed craters are very thin or nonexistent. Examples of young craters featuring above average ratio in their ejecta blankets are Haulani and Occator. Due to difficult illumination conditions toward higher latitudes, the quality of the color ratio data is limited and reliable only between approximately ±60° latitude.

[*Howett et al.*, 2011]. On Vesta no indication of nanophase iron was found, but instead, space weathering of the surface was influenced by continuous contamination of the regolith with carbonaceous chondrite-like material [*Pieters et al.*, 2016].

2. Data and Methods

2.1. Data

For this study we use two color ratio maps of Ceres, ratio F8 (438 nm)/F3 (749 nm) and ratio F8 (438 nm)/F5 (965 nm). The color data are photometrically corrected [*Schröder et al.*, 2014; *Schroeder et al.*, 2016] and provided at a resolution of 140 m/pixel [*Roatsch et al.*, 2016]. The meaning of the used ratios are described by *Stephan et al.* [2016] in detail and are discussed in comparison with the VIR instrument and with respect to spectral properties of the surface materials. Due to difficult illumination conditions toward the polar areas, this data set is reliable only between ~ ±60° latitude.

For each study area the color ratios are measured as the mean of all valid pixel ratios that are contained in the respective investigation area. The standard deviation in the according study area was calculated from the measured pixel ratio distribution.

2.2. Measurements of Crater Size-Frequency Distributions

The measurement and presentation of crater frequencies follows the general recommendations outlined by [*Arvidson*, 1979]. Model ages were determined from cumulative crater plots [*Michael et al.*, 2016]. The mapping of measurement areas and craters is performed with the CraterTools add-in [*Kneissl et al.*, 2011] for ArcGIS. Ceres appears to have been battered by secondary craters. Proximal secondary craters often form clusters of similar-sized craters. A quantitative analysis of the crater spatial randomness is applied to our crater measurements [*Michael et al.*, 2012]. Obvious crater clusters were excluded from the measurements, and if possible, such areas were completely excluded from the analysis. Thus, because we used the very same areas for the determination of the color ratios and surface ages, the area definition is based on both, the homogeneity of the color ratios and the character of the crater distribution, i.e., the absence of obvious secondary crater clusters.

2.3. Area Definition

We selected units which best reflect materials excavated from depth and distributed inside and outside the impact craters. The selected ratio range is not representative for extreme values above or below the average,

but chosen for good coverage of intermediate values, in order to derive reasonable data points for the color ratio-model age relationship. Due to the violent nature of impacts, it is possible that some material was either mixed with the original surface or excavated from different depths, resulting in an inhomogeneous pattern in the ratio data. These units were excluded, because the integrated spectral characteristics of the measurement area are not purely related to the time-dependent factor of spectral change. Therefore, only parts of ejecta blankets or melt pools with relatively homogenous spectral characteristics are used for the analysis. Also, outgassing events have been reported related to bright spots on Ceres [*Nathues et al*., 2015]. If fresh material from the bright spots precipitates onto the surface, the thin coating of fresh material would appear more juvenile than the geologic unit for which the frequency of impact craters is actually measured. Thus, we also excluded areas with any signs of such coating related to bright spots. For reliable CSFD measurements, it is also required that the selected areas are large enough for sufficient crater statistics and that craters are evenly distributed in space and are not obscured, e.g., by rough topography in parts of the area.

2.4. Absolute Model Ages

The cratering chronology of bodies inside the asteroid main belt is still debated by several groups following different approaches [*Hiesinger et al*., 2016; *O'Brien et al*., 2014; *Schmedemann et al*., 2014]. However, for the last 3 Ga, most groups consider the impactor flux to have been constant, although at different levels. Since the absolute ages of the presented measurements are all younger than 3 Ga, the different models of early solar system bombardment will not influence the results. The main difference between the two competing chronology systems is the shape of the applied crater production function. Thus, the derived ages are not simply offset by a fixed factor; they vary depending which crater diameter range is used for the investigation. Each measurement is given in the supporting information as a cumulative (Table S1 in the supporting information) and an R plot (Table S2) of the CSFD, including fitted isochrons for both chronology systems. Absolute ages are based on the chronology systems outlined in *Hiesinger et al.* [2016]. Hereafter, we refer to the chronology systems as LDM (lunar-derived model) [*Hiesinger et al*., 2016; *Schmedemann et al*., 2014] and ADM (asteroid-derived model) [*Hiesinger et al*., 2016; *O'Brien et al*., 2014].

3. Description of the Study Areas

Figure 2 gives an overview of the locations of the areas used in this study. Ikapati and Haulani craters show strong bluish characteristics and appear to be relatively young based on their pristine morphologies (Figure 3). Due to their youthful nature, the number of craters superimposed on their ejecta blankets is relatively small. Thus, we selected several smaller areas around these craters for better statistics. In addition, we use the multiple data points around these two craters to investigate the level of variability in the measured data. Due to their larger diameter, Ikapati and Haulani likely feature significantly thicker ejecta deposits inside the measured areas than smaller craters with similarly bluish characteristics, such as Oxo. In the case of Oxo, there is a high probability that the thin ejecta blanket does not fully cover the underlying material due to a regolith mixing from gardening due to subsequent cratering and insufficient blanketing effect of the ejecta itself. Impact gardening is less important for mixing thick ejecta deposits.

The spectral separation of filters F5 (965 nm) and F8 (438 nm) is larger than that of F3 (749 nm) and F8 (438 nm). Thus, it is expected that the color ratio is higher for F8/F5 than for F8/F3, if the change occurs over the full spectral range between F5 and F8, and not just between F8 and F3. A detailed analysis of the spectral behavior of the bluish material can be found in *De Sanctis et al.* [2016].

Table 1 lists information about the areas, model ages, and measured color ratios for each region. Groups of regions are numbered, such as Haulani 1–4. For Ikapati 1 and 2 we combined two individual areas of the same geologic unit that are separated by crater clusters. This procedure provides better statistics while leaving out obscuring geologic features, such as secondary/pit crater clusters. The cumulative crater reference frequency for craters $\geq$1 km, inferred from fitting the LDM or ADM crater production functions (N(1)), is not given for comparison between the two chronology systems, because the different shapes of the respective production functions do not allow a direct comparison.

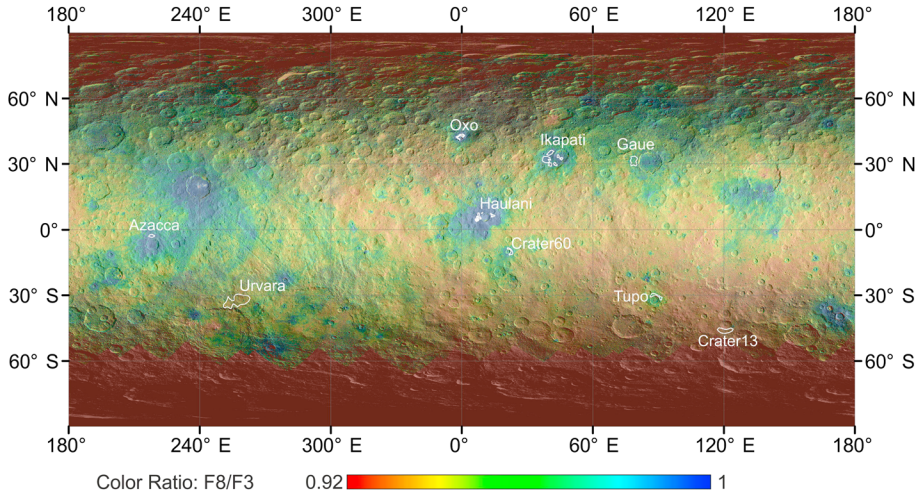

Figure 2. Color ratio F8 (438 nm)/F3 (749 nm) superimposed on clear filter data centered at the prime meridian. The distribution of color ratio data is similar to Figure 1. Analyzed areas are marked and annotated in white. For Ikapati and Haulani several areas are analyzed (detailed in Figure 3). Due to difficult illumination conditions toward higher latitudes, the quality of the color ratio data is reliable only between approximately ±60° latitude.

4. Results and Discussion

For the 16 analyzed areas, independent of the chronology models, one can clearly observe decreasing color ratios with increasing model age (Figure 4). For relatively old surfaces, the ADM gives younger model ages than the LDM. This is primarily related to the different shapes of the respective reference crater production functions that also influence the offset of the respective chronology functions. Because the slopes of the fitted power functions are steeper in the ADM, it results in a faster drop in color ratio values with increasing age than in the LDM. Furthermore, the ratio F8/F5 is characterized by a steeper drop of ratio values with increasing time if compared with the F8/F3 ratio in both chronology systems. This suggests that the change in spectral properties is not limited to the range either from F8 to F3 or from F3 to F5 but is acting over the full spectral range covered by the FC instrument.

In Figure 4 the data scatter over 1.3 standard deviations around the model functions. Color ratio measurements can be affected by the following issues:

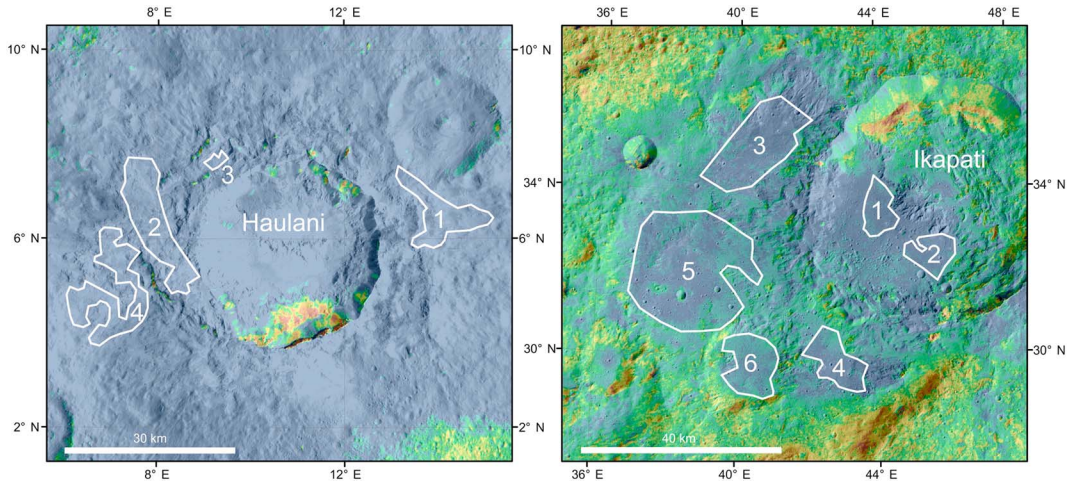

Figure 3. Clusters of investigation areas at craters Haulani (Ø ~ 34 km) and Ikapati (Ø ~ 50 km). Numbers indicate the individual areas listed in Table 1. Landslides at the crater rims mobilized "reddish" material that covers parts of the crater floors (see also the second issue in section 4). Both maps show the F8/F5 color ratio in the same range as in Figure 1.

Table 1. Areas, Spectral Ratios, and Cratering Model Ages of Study Regions[a]

Name	Area (km^2)	LDM (Ma)	LDM Positive Error (Ma)	LDM Negative Error (Ma)	ADM (Ma)	ADM Positive Error (Ma)	ADM Negative Error (Ma)	F8/F3	F8/F3 Error	F8/F5	F8/F5 Error
Azacca	240.30	75.9	15.0	15.0	45.8	5.0	5.0	1.017	0.012	1.079	0.012
Crater13	561.90	1330.0	270.0	270.0	272.0	41.0	41.0	0.928	0.026	0.968	0.027
Crater60	201.20	3.0	0.7	0.6	3.0	0.4	0.4	0.993	0.013	1.065	0.013
Gaue	758.70	162.0	21.0	21.0	64.5	5.2	5.2	0.975	0.024	1.027	0.025
Haulani 1	81.59	2.7	0.8	0.6	3.4	0.5	0.5	1.089	0.008	1.200	0.009
Haulani 2	125.90	2.2	0.6	0.5	3.1	0.4	0.4	1.087	0.010	1.199	0.011
Haulani 3	6.38	2.6	0.7	0.6	5.9	1.5	1.3	1.096	0.002	1.210	0.002
Haulani 4	117.80	1.7	0.2	0.2	2.8	0.4	0.4	1.084	0.010	1.197	0.010
Ikapati 1 and 2	186.60	19.2	2.2	2.2	19.4	1.9	1.9	1.012	0.010	1.073	0.011
Ikapati 3	207.80	42.0	8.3	8.3	34.5	2.5	2.5	1.011	0.014	1.077	0.015
Ikapati 4	83.71	43.1	9.9	8.6	29.8	4.1	4.1	1.010	0.009	1.069	0.009
Ikapati 5	457.30	66.4	10.0	10.0	34.3	3.1	3.1	1.000	0.021	1.061	0.022
Ikapati 6	113.30	21.9	3.0	3.0	25.1	2.4	2.4	1.000	0.010	1.054	0.010
Oxo	137.50	0.5	0.2	0.2	0.5	0.2	0.2	1.061	0.012	1.160	0.013
Tupo	274.60	48.3	6.5	6.5	35.9	3.0	3.0	0.968	0.016	1.021	0.017
Urvara	2505.00	242.0	16.0	16.0	110.0	7.2	7.2	0.947	0.049	0.990	0.051

[a]Errors given are the 1 sigma standard deviation of the measured values.

1. *Variable ejecta blanket thickness.* Small craters are surrounded by thinner ejecta blankets than large craters. For instance, Oxo is a relatively small crater (Ø ~ 10 km) whose ejecta blanket amounts to only about 4 m thickness averaged across the study area [*Housen and Holsapple*, 2011]. For comparison, the average ejecta thickness in the study area next to the 170 km diameter Urvara crater is about 50 m. Consequently and in agreement with *Werner and Medvedev* [2010], the color ratio of thin ejecta blankets from small craters may have been affected more efficiently by subsequent impact gardening due to mixing the underlying older reddish material into fresh bluish material. This mixing would shift the measured color ratio toward lower values.
2. *Inhomogeneous surface geology.* It might also be possible that the excavated material already had different than average spectral characteristics, which would support the idea of an inhomogeneous subsurface on Ceres [*Bland et al.*, 2016]. For example, it is possible that a relatively small crater excavated more bluish material close to a young large crater than it would have excavated far away from larger craters. This could be a common scenario due to the incorporation of material that was already excavated by the neighboring large crater. While the excavated subsurface material, deposited in the ejecta blanket of a midsized crater such as Haulani, has strong bluish characteristics, the material just below the deposited ejecta blanket is potentially more reddish. This situation is illustrated in Figure 3 where parts of the southern rim wall of Haulani including parts of the preimpact shallow subsurface material destabilized and moved downslope on the crater floor.

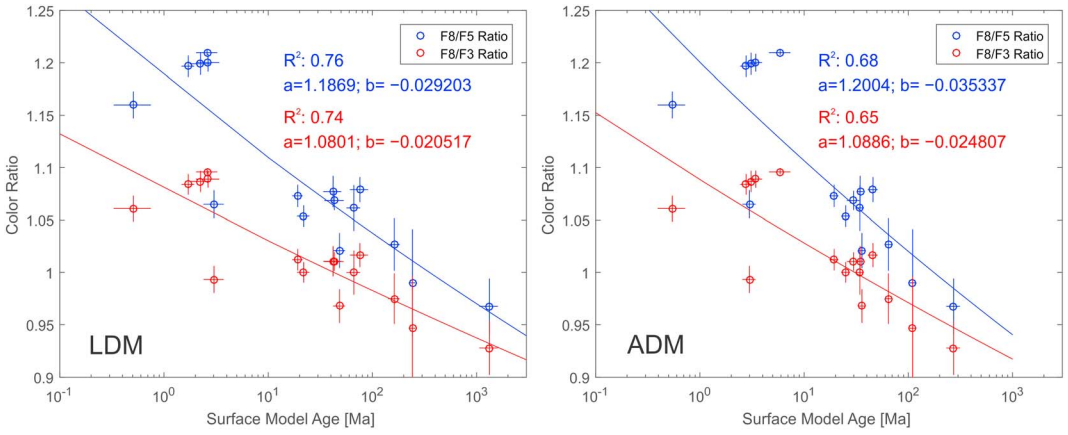

Figure 4. Measured color ratios versus absolute model ages for LDM and ADM. Coefficients for a power law fit ($y = ax^b$) are given for each fit as well as the respective squared residuals (R^2). Off-trend data points are within 1.3 standard deviations with respect to the model function and used for the fitting process.

3. *Coating*. Thin coatings of bluish material are clearly visible in the used color ratios, but they do not necessarily cover a potentially much older cratering record. This case is most obvious at the Kirnis crater southeast of Occator where the western half of Kirnis appears in bluish colors due to a thin blanketing that appears to originate at Occator, although crater frequencies in this area are very high, indicating an older age and no difference from the eastern part of Kirnis with a more reddish appearance (Figure 1).

4.1. Age Distribution in Haulani and Ikapati Cluster

Figure 3 is a close-up of the groups of measurement areas at craters Haulani and Ikapati. Within the error bars, all model ages outside the craters within each group are plausibly the same. Combined areas 1 and 2 inside Ikapati are about a factor of 2 younger than the absolute model ages outside Ikapati (~20 Ma versus ~40 Ma). *Neesemann et al.* [2016] found similar behavior at Occator crater (Figure 1). In case reasonably large impacts are able to trigger prolonged subsurface activity at the impact site, it has been suggested that the interior of both craters cooled at a slower rate than the thin ejecta blankets and thus, due to lower viscosity, recorded impact craters only after a while. Alternatively, it may be possible that the material in the crater interior has a higher strength than the material of the adjacent ejecta blankets leading to smaller crater sizes which finally might produce misleading model ages [*Dundas et al*., 2010; *van der Bogert et al*., 2010]. This hypothesis is somewhat weakened by the observation of flow features at Ikapati [*Krohn et al*., 2016a, 2016b], which suggest viscous flows of material from inside Ikapati into ponds outside the crater. Thus, we expect similar material properties for the ponds inside and outside the crater. The timing of the flow feature emplacement is unknown. Thus, either it could be impact related or it could also have occurred at some point after the impact as impact induced cryovolcanism. In both cases similar morphology and material properties might be possible. Occator (~92 km) is about twice as large in diameter as Ikapati (~50 km) and features several bright spots that may be indicative of very recent activity [*Nathues et al*., 2015]. The even larger crater Dantu (~120 km) [*Kneissl et al*., 2016; *Williams et al*., 2016] also shows bright spots near its southern crater rim associated with bluish material, which appears to be related to small impact craters, indicating a shallow reservoir of bluish material. The size of the spots is comparable to the highest available image resolution of about 35 m.

4.2. Low-Ratio Areas

The lowest color ratio values on Ceres across significant continuous areas are located immediately south and southwest of the Kerwan crater. If such a color ratio value represents the final state in the process leading to optical maturation, an analysis of respective surface ages does not contribute more information to the temporal dependence of the process, because the measured surface age could be older than the age when maturation has been reached. However, the observation implies that the area SSW Kerwan crater is one of the least resurfaced parts of Ceres where color ratios are available. The close proximity of Kerwan may further imply that the Kerwan impact event occurred earlier than the time interval required for the spectral change to happen. Otherwise, higher color ratios should be visible throughout the whole Kerwan ejecta blanket.

5. Conclusion

Our analysis shows the dependency of the spectral characteristics of recently exposed materials on the exposure time. The power law dependency between the measured color ratios and exposure ages found in this study may help to identify the process causing the optical maturation. Possible processes could be a change of grain sizes, similar to that observed for the Tiger stripes on Enceladus [*Jaumann et al*., 2008], or an outgassing of some kind of volatile substances, such as the dehydration of hydrated minerals or as cited for other bodies optical maturation due to exposure to micrometeorite bombardment and radiation. A variety of possibilities is discussed by *Stephan et al.* [2016]. Due to the observed strong dependence between the color ratio and surface exposure age, the presented color ratio maps may also serve as an indicator for relative surface ages. This is only a rough indication because the ratios at the surface are probably affected by the varying abundance of juvenile bluish material in the subsurface.

Acknowledgments
This work has been supported by the German Space Agency (DLR) on behalf of the Federal Ministry for Economic Affairs and Energy, Germany, grants 50 OW 1505 (N.S., T.K., and A.N.) and 50 QM 1301 (G.M.), and Helmholtz-Gemeinschaft (Helmholtz Association) PD-207 (K.K.). We thank the Dawn flight team for their excellent job of navigating and maintaining the probe and the reviewers Stephanie Werner and Carolyn van der Bogert for their constructive and valuable comments. The global color mosaics of Ceres and their respective description used in this study are available at http://sbn.psi.edu/archive/dawn/fc/certified/DWNCHFFC2_2/ Geometry data of the mapped areas and craters are listed in the supporting information Tables S3–S18. Alternatively, geometry data are also available from the lead author of this work.

References

Ammannito, E., et al. (2016), Distribution of phyllosilicates on the surface of Ceres, *Science*, *353*(6303), doi:10.1126/science.aaf4279.
Arvidson, R. (1979), Crater Analysis Techniques Working Group—Standard techniques for presentation and analysis of crater size-frequency data, *Icarus*, *37*(2), 467–474.

Bland, M. T., et al. (2016), Composition and structure of the shallow subsurface of Ceres revealed by crater morphology, *Nat. Geosci.*, *9*(7), 538–542.
Clark, R. N., et al. (2008), Compositional mapping of Saturn's satellite Dione with Cassini VIMS and implications of dark material in the Saturn system, *Icarus*, *193*, 372–386.
De Sanctis, M. C., et al. (2011), The VIR spectrometer, *Space Sci. Rev.*, *163*(1), 329–369.
De Sanctis, M. C., et al. (2016), Bright carbonate deposits as evidence of aqueous alteration on (1) Ceres, *Nature*, *536*(7614), 54–57.
Dundas, C. M., L. P. Keszthelyi, V. J. Bray, and A. S. McEwen (2010), Role of material properties in the cratering record of young platy-ridged lava on Mars, *Geophys. Res. Lett.*, *37*, L12203, doi:10.1029/2010GL042869.
Hapke, B. (1973), Darkening of silicate rock powders by solar wind sputtering, *Moon*, *7*(3), 342–355.
Hiesinger, H., et al. (2016), Cratering on Ceres: Implications for its crust and evolution, *Science*, *353*(6303), doi:10.1126/science.aaf4759.
Housen, K. R., and K. A. Holsapple (2011), Ejecta from impact craters, *Icarus*, *211*(1), 856–875.
Howett, C. J. A., J. R. Spencer, P. Schenk, R. E. Johnson, C. Paranicas, T. A. Hurford, A. Verbiscer, and M. Segura (2011), A high-amplitude thermal inertia anomaly of probable magnetospheric origin on Saturn's moon Mimas, *Icarus*, *216*(1), 221–226.
Jaumann, R., et al. (2008), Distribution of icy particles across Enceladus' surface as derived from Cassini-VIMS measurements, *Icarus*, *193*, 407–419.
Jaumann, R., et al. (2016), Age-dependent morphological and compositional variations on Ceres, in *Lunar and Planetary Science Conference*, pp. 1455, LPI Contribution, The Woodlands, Tex.
Kneissl, T., S. van Gasselt, and G. Neukum (2011), Map-projection-independent crater size-frequency determination in GIS environments—New software tool for ArcGIS, *Planet. Space Sci.*, *59*(11-12), 1243–1254.
Kneissl, T., et al. (2016), Geologic mapping of the Ac-H-3 Dantu Quadrangle of Ceres from NASA's Dawn Mission, in *Lunar and Planetary Science Conference*, pp. 1967, LPI Contribution, The Woodlands, Tex.
Krohn, K., et al. (2016a), Channels and cryogenic flow features on Ceres, in *Lunar and Planetary Science Conference*, pp. 2001, LPI Contribution, The Woodlands, Tex.
Krohn, K., et al. (2016b), Cryogenic flow features on Ceres—Implications for crater-related cryovolcanism, *Geophys. Res. Lett.*, doi:10.1002/2016GL070370.
Michael, G. G., T. Platz, T. Kneissl, and N. Schmedemann (2012), Planetary surface dating from crater size-frequency distribution measurements: Spatial randomness and clustering, *Icarus*, *218*(1), 169–177.
Michael, G. G., T. Kneissl, and A. Neesemann (2016), Planetary surface dating from crater size-frequency distribution measurements: Poisson timing analysis, *Icarus*, *277*, 279–285.
Nathues, A., et al. (2015), Sublimation in bright spots on (1) Ceres, *Nature*, *528*, 237–240.
Neesemann, A., T. Kneissl, N. Schmedemann, S. H. G. Walter, G. G. Michael, S. van Gasselt, H. Hiesinger, R. Jaumann, C. Raymond, and C. T. Russell (2016), Size-frequency distributions of km to sub-km sized impact craters on Ceres, in *Lunar and Planetary Science Conference*, pp. 2936, LPI Contribution, The Woodlands, Tex.
O'Brien, D. P., S. Marchi, A. Morbidelli, W. F. Bottke, P. M. Schenk, C. T. Russell, and C. A. Raymond (2014), Constraining the cratering chronology of Vesta, *Planet. Space Sci.*, *103*, 131–142.
Pieters, C. M., and S. K. Noble (2016), Space weathering on airless bodies, *J. Geophys. Res. Planets*, *121*, 1865–1884, doi:10.1002/2016JE005128.
Pieters, C. M., et al. (2016), Surface processes and space weathering on Ceres, in *Lunar and Planetary Science Conference*, pp. 1383, LPI Contribution, The Woodlands, Tex.
Prettyman, T. H., et al. (2011), Dawn's gamma ray and neutron detector, *Space Sci. Rev.*, *163*(1), 371–459.
Roatsch, T., E. Kersten, K.-D. Matz, F. Preusker, F. Scholten, R. Jaumann, C. A. Raymond, and C. T. Russell (2016), High-resolution Ceres High Altitude Mapping Orbit Atlas derived from Dawn Framing Camera images, *Planet. Space Sci.*, *129*, 103–107.
Ruesch, O., et al. (2016), Cryovolcanism on Ceres, *Science*, *353*(6303), doi:10.1126/science.aaf4286.
Sasaki, S., E. Kurahashi, C. Yamanaka, and K. Nakamura (2003), Laboratory simulation of space weathering: Changes of optical properties and TEM/ESR confirmation of nanophase metallic iron, *Adv. Space Res.*, *31*(12), 2537–2542.
Schmedemann, N., et al. (2014), The cratering record, chronology and surface ages of (4) Vesta in comparison to smaller asteroids and the ages of HED meteorites, *Planet. Space Sci.*, *103*, 104–130.
Schroeder, S., et al. (2016), Resolved spectrophotometric properties of the Ceres surface from Dawn Framing Camera images, paper presented at DPS 48 / EPSC 11 Joint meeting, Pasadena, Calif., 16–21 Oct.
Schröder, S. E., S. Mottola, K.-D. Matz, and T. Roatsch (2014), In-flight calibration of the Dawn Framing Camera II: Flat fields and stray light correction, *Icarus*, *234*, 99–108.
Sierks, H., et al. (2011), The Dawn Framing Camera, *Space Sci. Rev.*, *163*, 263–327.
Stephan, K., et al. (2016), The nature of Ceres' bluish material, Abstract 172084 presented at 2016 Fall Meeting, AGU.
van der Bogert, C. H., H. Hiesinger, A. S. McEwen, C. Dundas, V. Bray, M. S. Robinson, J. B. Plescia, D. Reiss, K. Klemm, and T. Lroc (2010), Discrepancies between crater size-frequency distributions on ejecta and impact melt pools at lunar craters: An effect of differing target properties?, paper presented at Lunar and Planetary Science Conference, The Woodlands, Tex.
Wehner, G. K. (1964), Sputtering effects on the lunar surface, in *The Lunar Surface Layer*, edited by J. W. Salisbury and P. E. Glaser, pp. 313–322, Academic Press, New York and London.
Werner, S. C., and S. Medvedev (2010), The Lunar rayed-crater population—Characteristics of the spatial distribution and ray retention, *Earth Planet. Sci. Lett.*, *295*(1–2), 147–158.
Williams, D. A., et al. (2016), Geologic mapping of the Ac-H-7 Kerwan Quadrangle of Ceres from NASA Dawn Mission, in *Lunar and Planetary Science Conference*, pp. 1522, LPI Contribution, The Woodlands, Tex.